

Contents lists available at [ScienceDirect](https://www.sciencedirect.com)

Optik

journal homepage: www.elsevier.com/locate/ijleo

Periodic surface nanostructures induced by orthogonal femtosecond laser pulses on tungsten

Hongzhen Qiao^a, Guo Liang^a, Fangjie Shu^a, Xiangli Wang^c, Wenjing Cheng^a,
Jie Liu^a, Meng Wang^a, Jianjun Yang^b

^a Engineering Research Center for Photoelectric Intelligent Sensing, Department of Physics, Shangqiu Normal University, Henan 476000, China

^b State Key Laboratory of Applied Optics, Changchun Institute of Modern Optics, Fine Mechanics and Physics, Chinese Academy of Sciences, Changchun 130033, China

^c College of Electrical Engineering, Northwest MinZu University, Lanzhou, Gansu 730030, China

ARTICLE INFO

Keywords:

surface nanostructure
crossed linear polarizations
temporal delay
ultrafast laser pulse

ABSTRACT

Three types of surface nanostructures are fabricated on tungsten by adjusting azimuth angle θ of YVO₄ birefringent crystal and laser parameters in experiment. Different surface structure morphologies are introduced and their features are investigated. The frequency characteristics of the three type laser-induced surface nanostructures are studied by the fast Fourier transformation (FFT). By varying the azimuth angle of YVO₄ crystal we can not only convert one-dimensional (1D) grating-like structures into two-dimensional (2D) surface structures, but also control the structural arrangement. Compared with traditional two-step sequential processing method, the dual orthogonal pulses generating through YVO₄ birefringent crystal can induce better periodical 1D grating-like structure. Moreover, the 2D microbumps are mainly dependent on the energy deposition effect from dual pulses. We also provide the underlying texturing mechanism of final periodic surface structures.

1. Introduction

Laser induced periodic surface structures (LIPSSs) show distinct advantages for their prospects in both basic research and industrial applications of micro/nano-structure devices [1–4]. Compared to lithography methods, femtosecond laser processing as a direct laser writing technique can be finished facily within one step [1–7]. It has become a powerful tool in the precise processing of nanostructures on all types of solid materials such as metals [1,5,6], semiconductors [2,7], and insulators [8]. Therefore, femtosecond laser technique has exhibited a large potential of wide application in colorization, solar cells, waveguides, and superhydrophobic characteristics [1–10]. A wide range of morphologies have been successfully created, such as periodic grating-like structures, microbumps, subwavelength triangle structures, bionic functional structures, etc [11–14].

Texturing large-area nanostructures is still a challenge, but is urgently demand. The formation mechanisms of different surface nanostructure morphology are also needed to be explored for well controlling key factors and create new structures in the future. Some researchers fabricated new laser-induced surface nanostructures by adjusting distributions of laser pulses in time and space [9,12–17]. Effects of surface nanostructures including the shape, material properties, and roughness factor have been studied. The formation mechanism of surface nanostructures was particularly explored. Several models have been proposed to explain the formation dynamics of laser-induced surface structures [18–20]. Among them, it has been mostly accepted that the interference between the incident pulse

E-mail addresses: qiaohongzhen8@163.com (H. Qiao), jjyang@ciomp.ac.cn (J. Yang).

<https://doi.org/10.1016/j.ijleo.2021.168354>

Received 18 September 2021; Received in revised form 14 November 2021; Accepted 15 November 2021

Available online 18 November 2021

0030-4026/© 2021 Elsevier GmbH. All rights reserved.

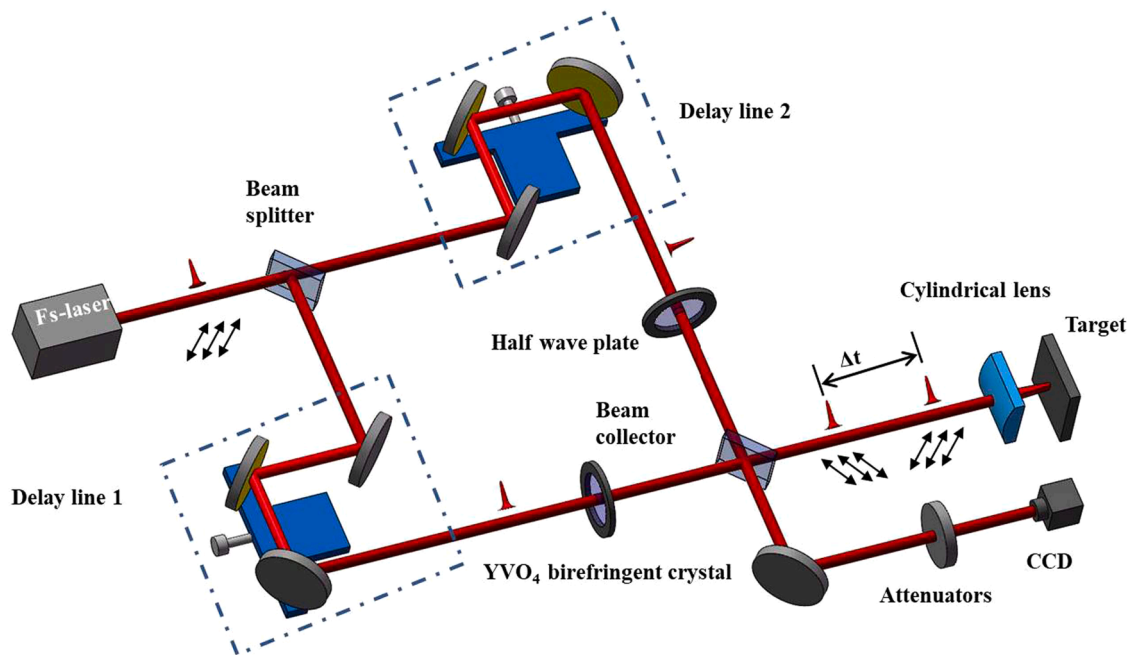


Fig. 1. Schematic diagrams of the experiment setup. Abbreviation: fs: femtosecond, Δt : the temporal delay of the two pulses, CCD: a charge coupled device. The double arrows represent directions of the linear polarization of femtosecond lasers.

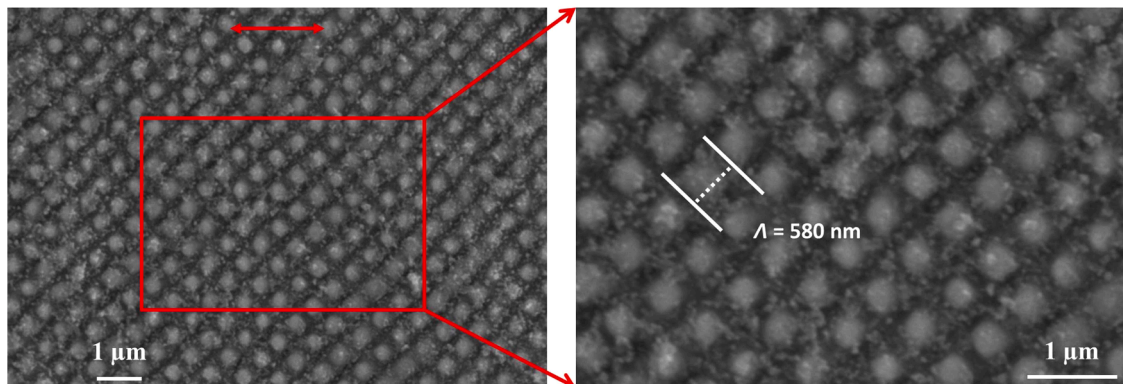


Fig. 2. (a) SEM images of 2D arrays of microbumps on tungsten surfaces induced by double femtosecond laser pulses at the total incident laser fluence of $F = 0.28 \text{ J/cm}^2$ and the sample scanning speed of $V = 0.03 \text{ mm/s}$. (b) The high-resolution SEM of 2D arrays of microbumps. The red double arrow represents the laser polarization direction. For interpretation of the references to color in this figure legend, the reader is referred to the web version of this article.

and the excited surface plasmon polariton (SPP) plays an important role in construction of LIPSSs on the surfaces of the targets [9,12,13,21]. The surface plasmon wavelength is approximately equal to the period of ripples which is always smaller than the laser wavelength in normal incidence [21]. But it is hard to explain the production of complex structure.

By rotating YVO₄ birefringent crystal, nanostructures were got on tungsten surfaces using dual femtosecond lasers with different azimuth angles. After FFT transformation of surface nanostructures patterns, we classified them into three types, 1D grating-like structures, 2D arrays of microbumps and aperiodic microbumps. Their periodic distribution characteristics can be clearly seen after FFT transformation. Further more, we explored the formation mechanism of surface nanomicrobumps and fabrication of 2D aperiodic microbumps. Both of them can be also reasonably explained by the energy deposition result of dual pulses.

2. Experiment

The experimental device is mainly composed of femtosecond laser source, beam splitter, YVO₄ birefringent crystal (the thickness of 1.26 mm and the diameter of 1 mm), plano-convex cylindrical lens, and target which is fixed on the three-dimensional precision

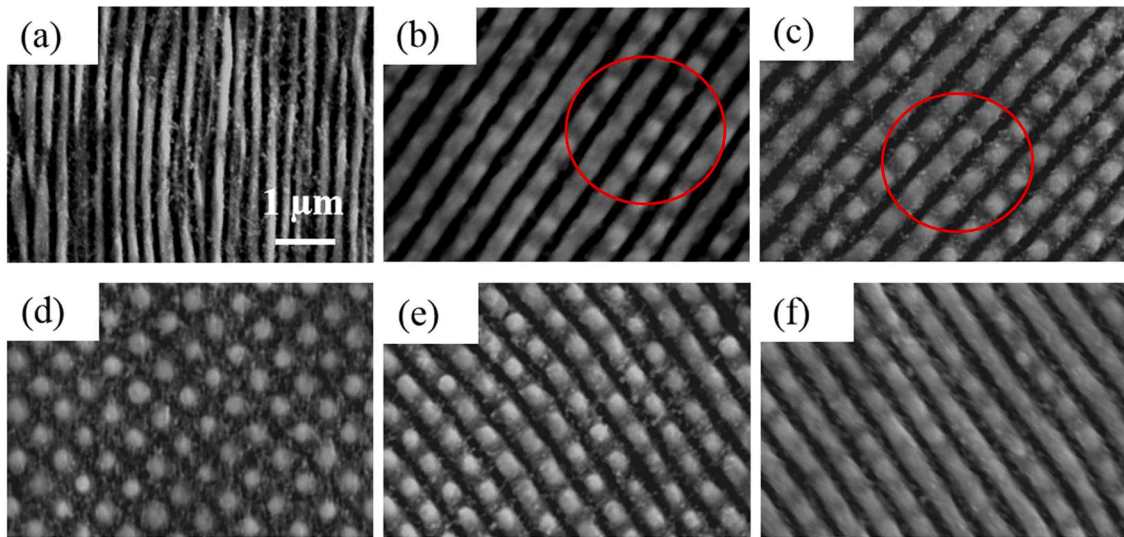


Fig. 3. Morphological evolution of the nanostructures on tungsten surfaces induced by femtosecond laser at the azimuth angle θ of (a) 0° , (b) 39° , (c) 43° , (d) 48° , (e) 53° and (f) 57° . For interpretation of the references to color in this figure, the reader is referred to the web version of this article.

moving translation stage (New Port UTM100 PPE1) in Fig. 1. A commercial Ti: sapphire laser amplifier system is used to generate linearly polarized 50 fs laser pulses with a maximum pulse energy 2 mJ at a repetition rate of 1 kHz with a central wavelength of 800 nm in air. As the schematic diagram in Fig. 1, a temporal delay of 1.2 ps is made between the two pulses. To structure tungsten surfaces, a mechanically polished tungsten plate (Goodfellow Co.) with a dimension size of $25 \times 25 \times 1 \text{ mm}^3$ and the purity of 99.95% serves as a material sample was irradiated by a fused plano-convex cylindrical lens with a focal length of $f = 50 \text{ mm}$. Before the experiment, the surface of material is polished by a fine grade of emery paper and degreased in acetone. The surface of sample is perpendicular to the optical axis. The sample is mounted on x–y–z translation stage (Newport UTM100 PPE1). Its translation direction is perpendicular to the line-shaped focal region. The scanning resolution is $1 \mu\text{m}$ and translating speed is within a range of 0.005–0.4 mm/s. The sample is positioned at the focused plane. The energy of the incident laser is attenuated through some neutral-density filters and measured before the cylindrical lens. Morphologies of the laser exposed surfaces were examined by scanning electron microscopy (SEM).

3. Results and discussions

In the experiment, the linearly polarized laser pulses were used as a light source with the pulse duration of 50 fs and a central wavelength of 800 nm at a 1 kHz repetition rate. The orthogonal pulses generated through a birefringent crystal of YVO_4 were focused on the polished tungsten surface by plano-convex cylindrical lens under normal incidence. A typical surface topography of 2D arrays of microbumps is shown in Fig. 2(a) at laser fluence about $F = 0.28 \text{ J/cm}^2$ at the azimuth angle $\theta = 48^\circ$. The directions of grooves distributed around the square lattices are completely different from the polarization of the linearly incident femtosecond laser from femtosecond laser source. From the magnified image in Fig. 2(b), it is seen that 2D arrays of microbumps are regularly generated in the center of square lattices on the sample surface. The metallic microbumps covered with scattered fragments around the grooves have a period of about $\Lambda = 580 \text{ nm}$ as shown in Fig. 2(b).

It is known that the azimuth angle θ of the YVO_4 birefringent crystal which could change the energy ratio of the double laser pulses and their directions with the orthogonal polarizations. As the azimuth angle θ increased, various grooved surface patterns were fabricated as shown in Fig. 3. Notably, the surface morphological characteristics of the nanostructures were greatly affected by the azimuth angle θ of the birefringent crystal. It is usually considered that the polarization of incident laser is perpendicular to the direction of grooves induced by laser on the tungsten surface [1,11], which can be confirmed by the typical result of Fig. 3(a). Compared with the grating-like in Fig. 3(a), the periods of regular groove structures in Fig. 3(b) and (f) are larger, and the ridges are much wider and smoother. Furthermore, we find that the size of scattered fragments around the grooves in Fig. 3(d) is bigger than others in Fig. 3. This phenomenon indicates that in the nonlinear process of the laser interaction with the material, there may be a strong ablation process in groove position. In contrast to 2D arrays of microbumps in Fig. 3(d), 2D aperiodic microbumps which are constituted by preferential grooves and messy grooves give distinct orientational preference as shown in Fig. 3(c) and (e). Changes in LIPSSs reflect changes of SPP. The etched grooves appear messy marks from a single vertical direction to a regular cross direction in Fig. 3(a) to (d), which also show that SPP induced by the laser on the surface of the material was deeply affected by the laser fluence. Several messy grooves are present as marked by the red circles in Fig. 3(b), (c). The most obvious phenomena of surface topography features in more details as shown in Fig. 3(b), (c), (e) and (f) imply that the preferential orientations of grooves are more likely to be determined by the polarization direction of the stronger laser pulse in the dual pulses.

In order to get the distribution law of the experiment quickly, the surface structure is studied by the two-dimensional FFT. We find

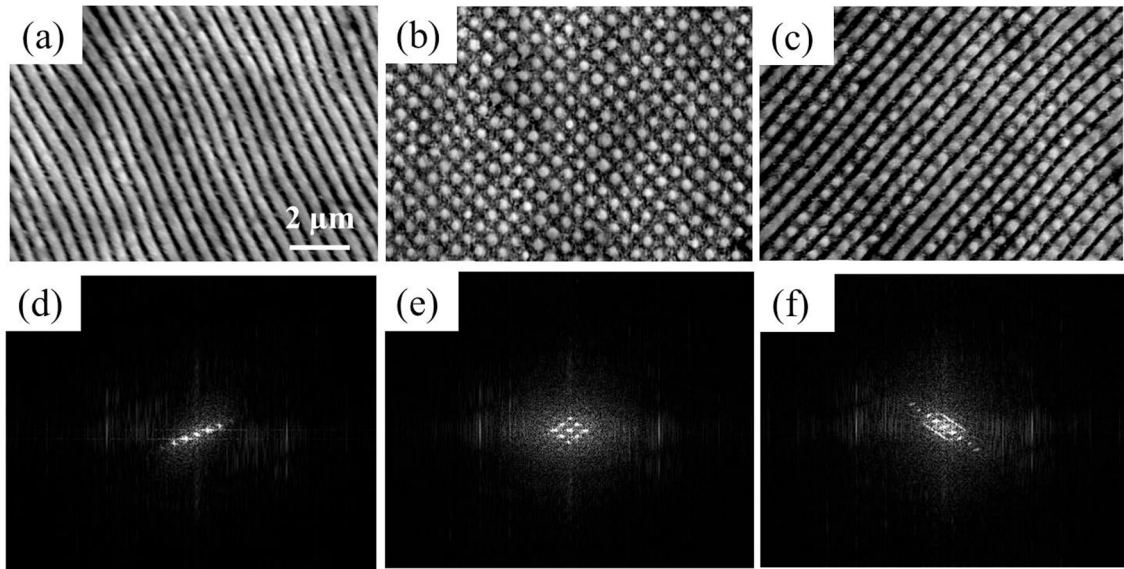


Fig. 4. Three types of microstructures: (a) SEM image of one-dimensional periodic grating-like structures. (b) SEM images of 2D arrays of microbumps. (c) SEM images of 2D aperiodic microbumps. (d), (e), and (f) are FFT of (a), (b), (c).

that there are three distinct types of 2D extended surface of microstructures provided in Fig. 4(a) to (c). Their corresponding FFT are shown in Fig. 4(d) to (f) where the bright spots indicate the homogeneity of the microbumps arrangement along different position and directions. Compared with Fig. 4(d), 2D aperiodic microbumps in Fig. 4(f) also have a dominant periodic from bottom right to top left which seems to be determined by the larger energy. However, the significant difference is that the weaker pulses still leave messy traces whose frequency is continuous in a special area shown in Fig. 4(f) but this is not seen in Fig. 4(d). According to previous researches, two types of periodic surface nanostructures have been reported by two laser pulses with perpendicular polarization directions: 1D periodic grating-like structure [11], 2D square lattice structure [13]. The formation mechanisms have been reported [12–17], but 2D aperiodic microbumps as shown in Fig. 4(c) induced by two pulses have been barely studied.

In order to reach the energy ratio of about 1.3 to formate 2D aperiodic microbumps in Fig. 3(e) the laser fluence of two laser pulses are given by $F_o = 0.19 \text{ J/cm}^2$ and $F_v = 0.15 \text{ J/cm}^2$, respectively. We design a two-step sequential processing method to study the fabrication of surface structures with different initial polarize pulse with large delay as shown in Fig. 5. In the experiment, the YVO₄ birefringent crystal was taken away in the laser path and the orientation of the 1D grating-like structures in Fig. 5(a) and (b) are perpendicular to the polarization directions of the linearly polarized laser at the scanning $V = 0.03 \text{ mm/s}$ through optical delay line 1 and delay line 2 in Fig. 1 at the normal incidence. First, we blocked the laser path of delay line 1 and released the laser in delay line 2 for five seconds to get 1D grating-like structures as shown in the right half of Fig. 5(c). Then we blocked the both arms and controlled the translation stage moved backward for two seconds. One minute later, we released the laser in delay line 1 to get the surface nanostructures of two lasers with large delay as shown in the left half in Fig. 5(c) and (e). To gain the insight of the two pulses affecting the formation of surface nanostructures, we changed the sequence of the two lasers and using the same method, and got the results as shown in the left half in Fig. 5(d) and (f). We find the nanostructures induced by the first beam were all eliminated. According to the results of one minute delay described above, it is found that the order of laser is the key to fabrication, and the polarization direction of the stronger laser does not determine the final orientations of grooves. This shows that the delay time is another important factor which can modulate the interaction result between the same incident laser and SPP.

The deposited energies relaxed to the lattice through electron-phonon processes often lasts tens of picoseconds for metals [13–16]. The previous studies have shown that the structures induced by the single beam femtosecond laser on the material surface are easily accompanied by the splitting phenomenon [21–24]. If one of the double laser pulses becomes stronger in the energy fluence, its deposition energies on the material surface will lead a serious ablation with the help of another pulse. In Ref. [13], we have already studied the delay dependence of nanostructures induced dual laser pulses on the tungsten surface and found there was a significantly correlated thermal melting induced by the two pulses within tens of picoseconds on tungsten. The phenomena in Fig. 3 can be physically analyzed as follows. The spatial period of the one-dimensional quasi-periodic grating-like structures in Fig. 3(a) is small, and the ridges are splitted obviously for one laser with higher energy. The ridges formed by the previous pulses are easily destroyed by the second pulse with same polarity. Compared with Fig. 3(a) 1D grating-like structures in Fig. 3(b) and (f) seem to be induced by the stronger laser pulse and have stable periodic. The ridges get significantly flatter and there is no division on the ridges. Furthermore, irregularly shaped microbumps on the ridges at the azimuth angle $\theta = 43^\circ$ or 53° can be found with different patterns of orientation preferences and there are no division on the ridges too. These results indicates that the surface dynamic of each pulse pair interacting with the material are related and coupled with each other, thereby avoiding the laser pulse from triggering a locally enhanced electric field on the ridges induced by the other pulses. So we can find the square lattices of metallic microbumps could be fabricated for the

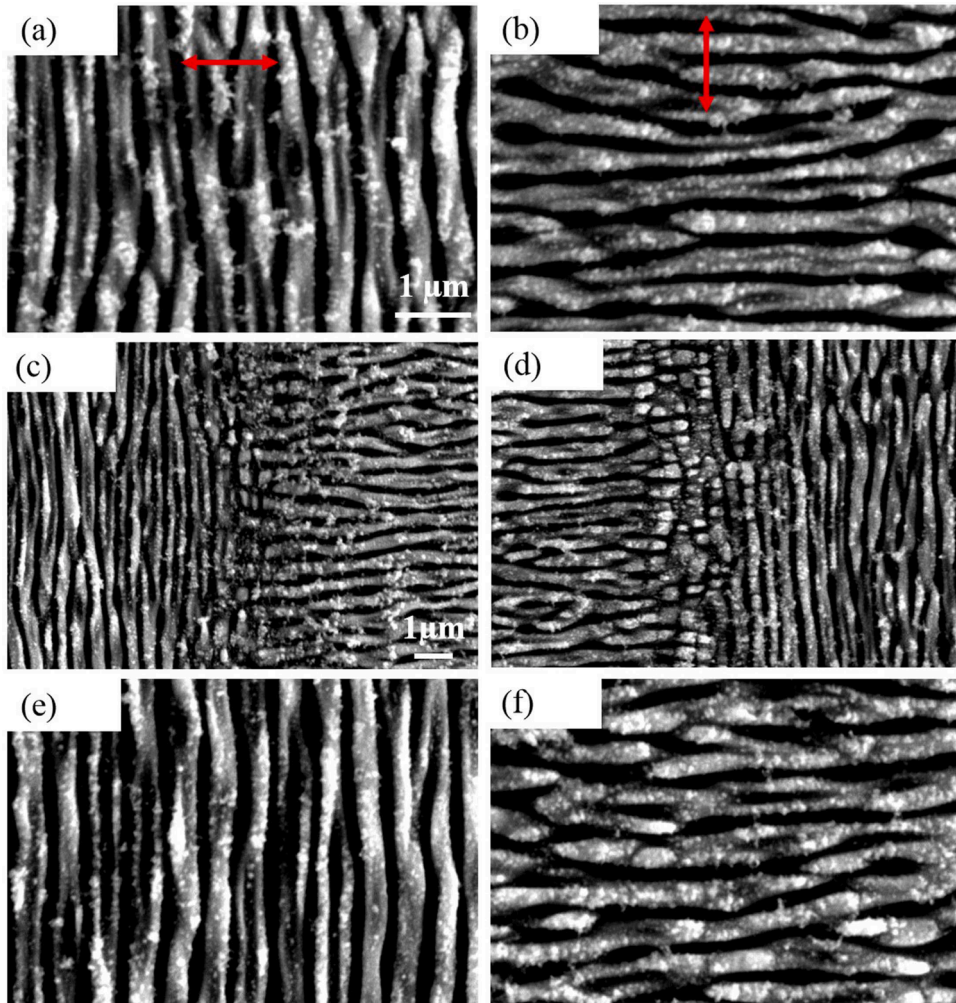


Fig. 5. (a), (b) 1D quasi-periodic grating-like structures fabricated with laser fluence F_0 and F_1 , respectively. The double arrows of (a) and (b) shown in red are polarization of double laser. (c), (d) 1D quasi-periodic grating-like structures fabricated at junction by two-step sequential processing method. (e), (f) The surface nanostructures are induced by two lasers with two-step sequential processing method. For interpretation of the references to color in this figure legend, the reader is referred to the web version of this article.

correlated thermal melting in tempo-spatial correlation induced by the two laser pulses.

4. Conclusions

In summary, we present a one-step processing method to directly obtain three types of nanostructures on the hard surfaces of tungsten by changing the azimuth angle θ of the birefringent crystal YVO_4 . After classification, they are attributed into three types of nanostructures: 1D grating-like structures, 2D arrays of microbumps and aperiodic microbumps. Although the morphological characteristics of three types of nanostructures can be changed by the adjusted optical axis of the crystal, it is difficult to obtain the same effect if the temporal-delay of double pulses increased into one minute. We analyze the morphological characteristics of the three types of nanostructures by FFT and design a large temporal-delay experiment in the two-step method to explore the reason for the fabrication of 2D aperiodic microbumps obtained by YVO_4 .

Declaration of Competing Interest

The authors declare that they have no known competing financial interests or personal relationships that could have appeared to influence the work reported in this paper.

Acknowledgments

We acknowledge financial supports from National Natural Science Foundation of China (Nos. 11674178, 11764036, 12004238), Natural Science Foundation of Henan Province (Nos. 182102210484, 18A416003).

References

- [1] A.Y. Vorobyev, V.S. Makin, C.L. Guo, Brighter light sources from black metal: significant increase in emission efficiency of incandescent light sources, *Phys. Rev. Lett.* 102 (2009), 234301.
- [2] J.J. Nivas, S. Amoroso, Generation of supra-wavelength grooves in femtosecond laser surface structuring of silicon, *Nanomaterials* 11 (2021) 174.
- [3] A.A. Bushunov, A.A. Teslenko, M.K. Tarabrin, V.A. Lazarev, S.I. Lobanov, Fabrication of antireflection microstructures on the surface of gas crystal by single-pulse femtosecond laser ablation, *Opt. Lett.* 45 (2020) 5994–5997.
- [4] G. Ye, W. Wang, D. Fan, P. He, Effects of femtosecond laser micromachining on the surface and substrate properties of poly-lactic acid (PLA), *Appl. Surf. Sci.* 538 (2021), 148117.
- [5] J.C. Wang, C.L. Guo, Ultrafast dynamics of femtosecond laser-induced periodic surface pattern formation on metals, *Appl. Phys. Lett.* 87 (2005), 251914.
- [6] M.S. Ahsan, M.S. Lee, Colorizing mechanism of brass surface by femtosecond laser induced microstructures, *Optik* 124 (18) (2013) 3631–3635.
- [7] K. Lou, S.X. Qian, X.L. Wang, Y. Li, B. Gu, C. Tu, H.T. Wang, Two-dimensional microstructures induced by femtosecond vector light fields on silicon, *Opt. Express* 20 (2012) 120–127.
- [8] C. Hnatovsky, V. Shvedov, W. Krolikowski, A. Rode, Revealing local field structure of focused ultrashort pulses, *Phys. Rev. Lett.* 106 (2011), 123901.
- [9] L. Jiang, A.D. Wang, B. Li, T.H. Cui, Y.F. Lu, Electrons dynamics control by shaping femtosecond laser pulses in micro/nanofabrication: modeling, method, measurement and application, *Light Sci. Appl.* 7 (2018) 17134.
- [10] J.L. Yong, F. Chen, Q. Yang, U. Farooq, X. Hou, Photoinduced switchable underwater superoleophobicity–superoleophilicity on laser modified titanium surfaces, *J. Mater. Chem. A* 2 (2014) 5499–5507.
- [11] L. Xue, J.J. Yang, Y. Yang, Y.S. Wang, X.N. Zhu, Creation of periodic subwavelength ripples on tungsten surface by ultra-short laser pulses, *Appl. Phys. A* 109 (2012) 357–365.
- [12] S. Hohm, A. Rosenfeld, J. Kruger, J. Bonse, Continuous modulations of femtosecond laser-induced periodic surface structures and scanned line-widths on silicon by polarization changes, *Opt. Express* 21 (2013) 15505–15513.
- [13] H.Z. Qiao, J.J. Yang, F. Wang, Y. Yang, J.L. Sun, Femtosecond laser direct writing of large-area two-dimensional metallic photonic crystal structures on tungsten surfaces, *Opt. Express* 23 (2015) 26617–26627.
- [14] Q. Liu, N. Zhang, J.J. Yang, H.Z. Qiao, Direct fabricating large-area nanotriangle structure arrays on tungsten surface by nonlinear lithography of two femtosecond laser beams, *Opt. Express* 26 (2018) 11718.
- [15] J.M. Romano, A. Garcia-Giron, P. Penchev, S. Dimov, Triangular laser-induced submicron textures for functionalising stainless steel surfaces, *Appl. Surf. Sci.* 440 (2018) 162–169.
- [16] D.W. Müller, T. Fox, P.G. Grützmacher, S. Suarez, F. Mücklich, Applying ultrashort pulsed direct laser interference patterning for functional surfaces, *Sci. Rep.* 10 (2020) 1–14.
- [17] A.S. Jalil, J.J. Yang, M. Elkabbash, C. Cong, C.L. Guo, Formation of controllable 1D and 2D periodic surface structures on cobalt by femtosecond double pulse laser irradiation, *Appl. Phys. Lett.* 15 (2019), 031601.
- [18] J. Reif, O. Varlamova, F. Costache, Femtosecond laser induced nanostructure formation: self-organization control parameters, *Appl. Phys. A* 92 (2008) 1019–1024.
- [19] M. Straub, M. Afshar, D. Feili, H. Seidel, K. König, Surface plasmon polariton model of high-spatial frequency laser-induced periodic surface structure generation in silicon, *J. Appl. Phys.* 111 (2012), 124315.
- [20] X.J. Wu, T.Q. Jia, F.L. Zhao, M. Huang, N.S. Xu, H. Kuroda, Z.Z. Xu, Formation mechanisms of uniform arrays of periodic nanoparticles and nanoripples on 6H-SiC crystal surface induced by femtosecond laser ablation, *Appl. Phys. A* 86 (2007) 491–495.
- [21] M. Huang, F.L. Zhao, Y. Cheng, N. Xu, Z.Z. Xu, Origin of laser-induced near-subwavelength ripples: interference between surface plasmons and incident laser, *ACS Nano* 3 (2009) 4062–4070.
- [22] M. Huang, Y. Cheng, F.L. Zhao, Z.Z. Xu, The significant role of plasmonic effects in femtosecond laser-induced grating fabrication on the nanoscale, *Ann. Phys.* 525 (2013) 74–86.
- [23] S. Hohm, A. Rosenfeld, J. Kruger, J. Bonse, Laser-induced periodic surface structures on titanium upon single-and two-color femtosecond double-pulse irradiation, *Opt. Express* 23 (2015) 15505–15513.
- [24] S. Sakabe, M. Hashida, S. Tokita, S. Namba, K. Okamuro, Mechanism for self-formation of periodic grating structures on a metal surface by a femtosecond laser pulse, *Phys. Rev. B* 79 (2009), 033409.